

Tetrathiafulvalene and Tetramethyltetraselenafulvalene Salts with $[M(\text{dcdmp})_2]$ Anions ($M = \text{Au}, \text{Cu}, \text{and Ni}$): High Conductivity and Unusual Stoichiometries

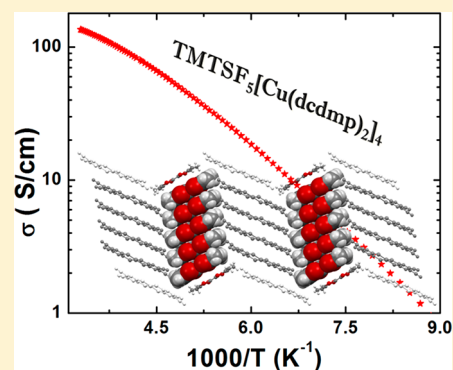
Rafaela A. L. Silva,[§] Isabel C. Santos,[§] Vasco Gama,[§] Elsa B. Lopes,[§] Pascale Auban-Senzier,[‡] Manuel Almeida,[§] and Dulce Belo^{*,§,¶}

[§]C²TN, Centro de Ciências e Tecnologias Nucleares, Instituto Superior Técnico, Universidade de Lisboa, E.N. 10 ao km 139.7, 2695-066 Bobadela LRS, Portugal

[‡]Laboratoire de Physique des Solides UMR 8502, CNRS-Université Paris-Sud, 91405 Orsay, France

Supporting Information

ABSTRACT: Four new charge transfer salts based on tetrathiafulvalene (TTF) or tetramethyltetraselenafulvalene (TMTSF) donors and transition metal complexes $[M(\text{dcdmp})_2]$ ($\text{dcdmp} = 2,3\text{-dicyano-5,6-dimercaptopyrazine}$), $\text{TMTSF}_5[\text{Cu}(\text{dcdmp})_2]_4$ (1), $(\text{TMTSF})_2[\text{Ni}(\text{dcdmp})_2]$ (2), and $(\text{TTF})_7[M(\text{dcdmp})_2]_6$ ($M = \text{Au}$ (3) and Cu (4)) were prepared by electrocrystallization. These compounds are characterized by a rich variety of crystal structures with unusual donor/acceptor stoichiometries. In spite of the uncommon structural types observed, these salts can be highly conducting. Compound 1 crystallizes with segregated TMTSF stacks, showing 1D metallic properties with a room temperature conductivity of 134 S/cm. Compound 2 crystallizes in an out-of-registry mixed column arrangement of donor dimers and acceptors. Compounds 3 and 4 appear in single crystal X-ray diffraction as isostructural and composed of columns of TTF hexamers that are disrupted by a single TTF layer and surrounded by $[M(\text{dcdmp})_2]^-$ monoanionic pairs, aligning perpendicularly to the hexamer stacks. However, measurements of the electric transport properties in single crystals suggest the existence of two phases. While phase 2 has a semiconducting behavior, phase 1 is clearly more conductive with copper complex 4 presenting a metal semiconductor transition around 210 K and room temperature conductivity of ~ 210 S/cm.



INTRODUCTION

Since the discovery of metallic behavior in tetrathiafulvalene (TTF)–tetracyano-*p*-quinodimethane (TCNQ)¹ and superconductivity in $(\text{TMTSF})_2\text{PF}_6$ ² (TMTSF = tetramethyltetraselenafulvalene), the first examples of organic metals and superconductors, respectively, these TTF and TMTSF molecules have been widely explored as building blocks for new molecular conductors, through their combination with a large variety of anions and acceptor molecules.^{3–8} It is now well established that high electrical conductivity and metallic properties can be achieved by the regular arrangement with extended networks in the solid state of partially oxidized donor molecules with strong HOMO–HOMO interactions, leading to partially filled electronic bands. This has been achieved in many salts of these donors with different monoanions, presenting a donor to acceptor stoichiometry of 2:1. Although not so frequently, other stoichiometries different from 2:1 have also been observed, but with a few exceptions, usually being associated with less conducting properties due to the nonuniformity of the intermolecular electronic interactions.^{3,7–10}

In spite of the large number of anions that have been combined with these donors, including several transition metal

bisdithiolene complexes, those based on the 2,3-dicyano-5,6-dimercaptopyrazine (dcdmp) ligand $[M(\text{dcdmp})_2]$ ($M = \text{Au}, \text{Cu}, \text{Pd}, \text{and Ni}$), have been less explored. Dithiolene ligands with nitrogen as heteroatoms, such as in pyrazine moieties, have been extensively used to explore their capability to establish side interactions or coordinate other metals.^{11–14}

Previous attempts to combine TTF or TMTSF with $[M(\text{dcdmp})_2]$ anions, were already described, however often without a description of the crystal structures of the salts obtained.¹⁵ For $M = \text{Au}$, highly conducting salts both with TTF and TMTSF were obtained presenting room temperature conductivities measured in single crystals of 100 and 13.4 S/cm respectively, but no crystal structure information could be obtained.¹⁵ Tomura et al. originally reported the preparation of $[M(\text{dcdmp})_2]$ complexes, with $M = \text{Pd}$ and Ni and described the structures of TTF salts with a 5:2 donor to acceptor stoichiometry and a poor semiconducting behavior with room temperature conductivities in the range $\sigma_{\text{RT}} = 10^{-2}\text{--}10^{-3}$ S/cm.¹⁶ More recently, a semiconducting family of salts,

Received: July 19, 2019

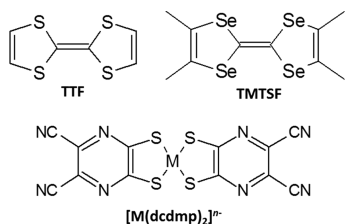
Revised: August 27, 2019

Published: September 10, 2019

combining these type of anions with thiophenic-TTF donors, has been reported with some exhibiting polymorphism.¹⁷

In this paper, we report results from further exploring TTF and TMTSF salts with $[M(\text{dcdmp})_2]$ complexes ($M = \text{Au}, \text{Cu}$, and Ni), leading to novel crystal structures with unusual stoichiometries and high electrical conductivities.

Scheme 1. Chemical Structures of Electron Donors TTF and TMTSF and Metal Bisdithiolene Anion



EXPERIMENTAL SECTION

General Methods. TMTSF and TTF were commercially obtained and used without any further purification. $(n\text{-Bu}_4\text{N})[M(\text{III})(\text{dcdmp})_2]$ ($M = \text{Au}$ and Cu)^{18,19} and $(n\text{-Bu}_4\text{N})_2[\text{Ni}(\text{II})(\text{dcdmp})_2]$ ¹⁶ were prepared following previously described procedures. Electrocrystallization was performed in H-shaped two-compartment cells separated by frit glass with Pt electrodes and under galvanostatic conditions. All solvents were purified following standard procedures²⁰ and freshly distilled immediately before their use.

Synthesis of $\text{TMTSF}_5[\text{Cu}(\text{dcdmp})_2]_4$ (1). Crystals were obtained by electrocrystallization at 30 °C, from an acetonitrile solution (20 mL) of $(n\text{-Bu}_4\text{N})[\text{Cu}(\text{III})(\text{dcdmp})_2]$ (2.3×10^{-3} M) and TMTSF (9.0×10^{-4} M). The electrocrystallization cell was sealed under nitrogen and after 18 days, using a current density of $1.0 \mu\text{A}\cdot\text{cm}^{-2}$, black, needle-shaped crystals were collected.

Synthesis of $\text{TMTSF}_2[\text{Ni}(\text{dcdmp})_2]_2$ (2). Crystals were obtained by electrocrystallization at 30 °C, from an 1,1,2-trichloroethane solution (25 mL) of $(n\text{-Bu}_4\text{N})_2[\text{Ni}(\text{II})(\text{dcdmp})_2]$ (9.0×10^{-4} M) and TMTSF (1.6×10^{-3} M). The electrocrystallization cell was sealed under nitrogen and after 25 days, applying a current density of $0.5 \mu\text{A}\cdot\text{cm}^{-2}$, dark-brown, needle-shaped crystals were collected.

Synthesis of $\text{TTF}_m[\text{Au}(\text{dcdmp})_2]_n$ (3). Crystals were obtained at room temperature by electrocrystallization from an acetonitrile solution (18 mL) of $(n\text{-Bu}_4\text{N})[\text{Au}(\text{III})(\text{dcdmp})_2]$ (1.2×10^{-3} M) and TTF (2.0×10^{-3} M). The electrocrystallization cell was sealed under nitrogen and after 18 days, by applying a current density of $2 \mu\text{A}\cdot\text{cm}^{-2}$, dark-brown crystals with a metallic shine and well-defined parallelepiped shape were collected.

Synthesis of $\text{TTF}_m[\text{Cu}(\text{dcdmp})_2]_n$ (4). Crystals were obtained by electrocrystallization at 30 °C, from an acetonitrile solution (20 mL) of $(n\text{-Bu}_4\text{N})[\text{Cu}(\text{III})(\text{dcdmp})_2]$ (2.3×10^{-3} M) and TTF (1.3×10^{-3} M). The electrocrystallization cell was sealed under nitrogen and after 18 days, by applying a current density of $1.0 \mu\text{A}\cdot\text{cm}^{-2}$, black needle shaped crystals were collected.

X-ray Crystallography. X-ray diffraction studies were performed with a Bruker APEX-II CCD detector diffractometer using graphite monochromated $\text{MoK}\alpha$ radiation ($\lambda = 0.71073$ Å), in the φ and ω scans mode. A semiempirical absorption correction was carried out using SADABS.²¹ Data collection, cell refinement, and data reduction were done with the SMART and SAINT programs.²² X-ray data for the $(\text{TMTSF})_2[\text{Ni}(\text{dcdmp})_2]$ compound was collected using synchrotron radiation at Beamline ID11 ($\lambda = 0.40660$ Å, ESRF,

Table 1. Crystal and Refinement Data for $\text{TMTSF}_5[\text{Cu}(\text{dcdmp})_2]_4$ (1), $\text{TMTSF}_2[\text{Ni}(\text{dcdmp})_2]_2$ (2), $\text{TTF}_7[\text{Au}(\text{dcdmp})_2]_6$ (3), and $\text{TTF}_7[\text{Cu}(\text{dcdmp})_2]_6$ (4)^a

compound	$\text{TMTSF}_5[\text{Cu}(\text{dcdmp})_2]_4$ (1)	$\text{TMTSF}_2[\text{Ni}(\text{dcdmp})_2]_2$ (2)	$\text{TTF}_7[\text{Au}(\text{dcdmp})_2]_6$ (3)	$\text{TTF}_7[\text{Cu}(\text{dcdmp})_2]_6$ (4)
formula	$\text{C}_{49}\text{H}_{30}\text{Cu}_2\text{N}_{16}\text{S}_8\text{Se}_{10}$	$\text{C}_{32}\text{H}_{24}\text{NiN}_8\text{S}_4\text{Se}_8$	$\text{C}_{57}\text{H}_{14}\text{Au}_3\text{N}_{24}\text{S}_{26}$	$\text{C}_{57}\text{H}_{14}\text{Cu}_3\text{N}_{24}\text{S}_{26}$
molec mass	2016.05	1339.22	2459.38	2059.10
T (K)	296(2)	295(2)	150(2)	150(2)
λ (nm)	0.71073	0.40660	0.71073	0.71073
dimens (mm)	$0.50 \times 0.05 \times 0.02$	$0.08 \times 0.03 \times 0.01$	$0.20 \times 0.03 \times 0.02$	$0.30 \times 0.04 \times 0.02$
crystal color	black	dark green	brown	black
crystal system	triclinic	monoclinic	triclinic	triclinic
space group	$P\bar{1}$	$P2_1/c$	$P\bar{1}$	$P\bar{1}$
a (Å)	12.4628(5)	28.712(6)	12.7916(9)	12.7105(6)
b (Å)	15.0274(5)	13.498(3)	16.1384(11)	16.2090(8)
c (Å)	18.5723(7)	10.631(2)	21.3088(16)	20.9179(9)
α (deg)	111.581(2)	90.00	98.695(2)	97.343(2)
β (deg)	95.596(2)	90.69(3)	106.708(2)	104.853(2)
γ (deg)	102.480(3)	90.00	110.876(3)	111.324(3)
volume (Å ³)	3041.7(11)	4119.7(14)	3775.2(5)	3761.7(3)
Z	2	4	2	2
ρ_{calc} (g·cm ⁻³)	2.162	2.159	2.164	1.818
h, k, l range	$\pm 15, -17/+18, -21/+19$	$\pm 32, \pm 15, \pm 11$	$-14/+15, -18/+19, \pm 25$	$-15/+12, -17/+19, \pm 25$
θ_{max} (deg)	25.68	13.36	25.681	25.681
refln collected	32919	22469	28429	45507
unique refln	10301 [$R_{\text{int}} = 0.0572$]	5724 [$R_{\text{int}} = 0.0819$]	13970 [$R_{\text{int}} = 0.0917$]	13485 [$R_{\text{int}} = 0.1935$]
refln $> 2\sigma(I)$	4556	3336	8326	4036
data/restraints/parameters	10301/6/776	5724/117/478	13970/18/991	13485/0/991
GOF on F^2	0.908	1.186	0.893	0.865
R_1	0.0546	0.0879	0.0539	0.0890
ωR_2	0.1201	0.1468	0.0869	0.1806
largest diff peak and hole (e·Å ⁻³)	0.841 and -0.662	0.816 and -0.658	1.345 and -1.257	0.809 and -0.796

^aCrystallographic data for 1–4 were deposited with the Cambridge Crystallographic Data Centre with CCDC nos. 1940745–1940748, respectively.

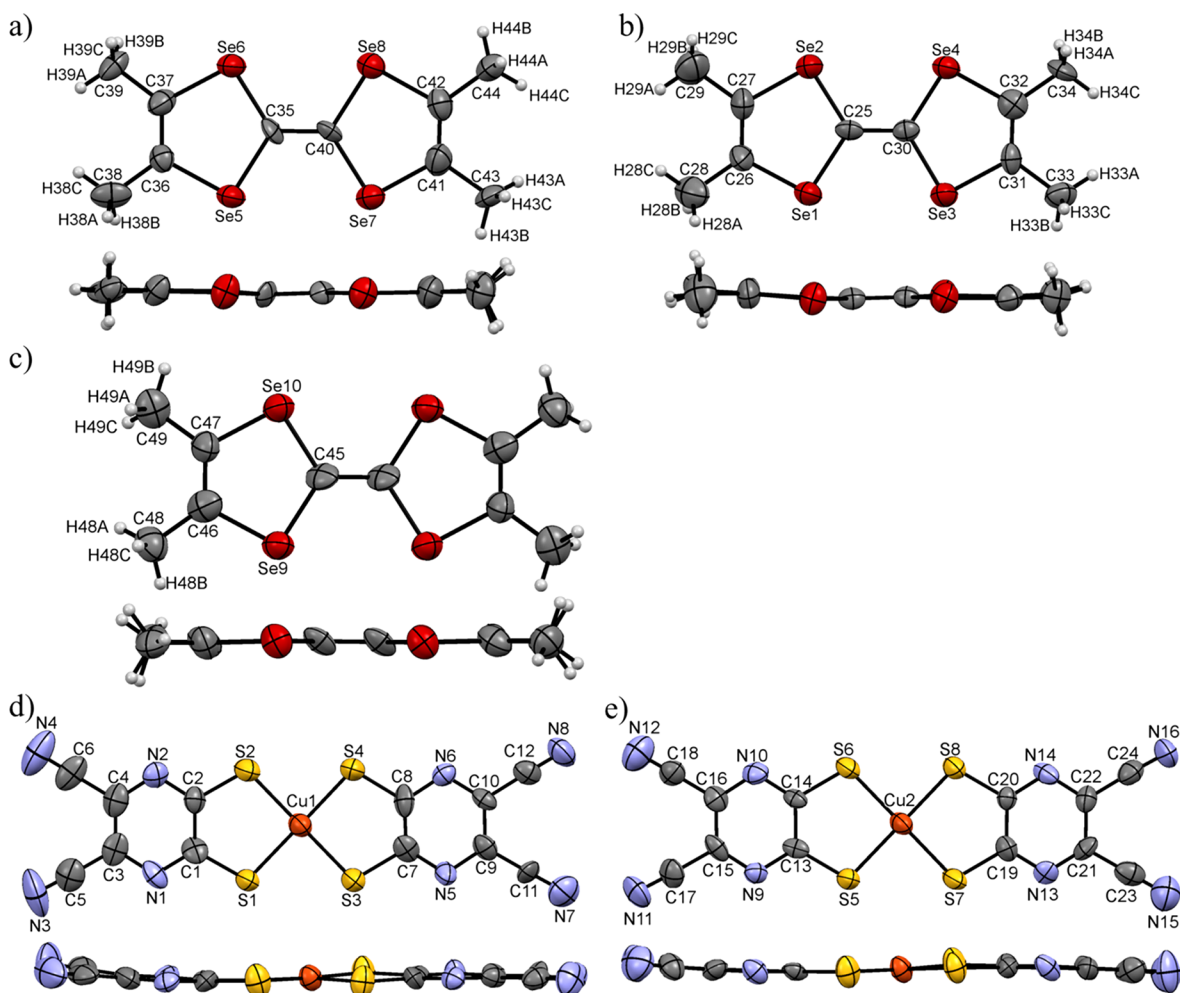


Figure 1. ORTEP and atomic numbering schemes (top and side views) of TMTSF donor molecules A (a), B (b), and C (c) and acceptor $[\text{Cu}(\text{dcdmp})_2]$ molecules D (d) and E (e) in the crystal structure of $(\text{TMTSF})_5[\text{Cu}(\text{dcdmp})_2]_4(\mathbf{1})$, with thermal ellipsoids drawn at the 70% probability level.

Grenoble, France) on a Enraf-Nonius CAD4- diffractometer in a ω - 2θ scan mode. Data collection, cell refinement, and data reduction were done with CAD4 software programs. The intensities were corrected for Lorentz, polarization, and absorption effects by empirical corrections based on psi-scans using the Enraf-Nonius reduction program, MoIEN.²³ The structures were solved by direct methods using SIR97²⁴ and refined by fullmatrix least-squares methods using the program SHELXL97²⁵ using the winGX software package.²⁶ Non-hydrogen atoms were refined with anisotropic thermal parameters, whereas H-atoms were placed in idealized positions and allowed to refine riding on the parent C atom. Molecular graphics were prepared using Mercury.²⁷

Intermolecular Energy Interactions Calculations. The interaction energies were calculated with freeware PrimeColor Software, CAESAR.²⁸ The program employs the extended Hückel method^{29–31} where the basis set consists of Slater type orbitals of double- ζ quality. The exponents, contraction coefficients, and atomic parameters were taken from previous work.³²

Electrical Transport Properties. Electrical conductivity and the thermoelectric power measurements were made along the needle axis of the crystals in the temperature range of 50–320 K, using a measurement cell attached to the cold stage of a closed cycle helium refrigerator. In the first step, the thermopower was measured by using a slow AC (ca. 10^{-2} Hz) technique,³³ by attaching two $\theta = 25 \mu\text{m}$ diameter 99.99% pure Au wires (Goodfellow), thermally anchored to two quartz blocks, with Pt paint (Demetron 308A) to the extremities of an elongated sample as in a previously described apparatus,³⁴

controlled by a computer.³⁵ The oscillating thermal gradient was kept below 1 K and was measured with a differential Au-0.05 atom % Fe versus chromel thermocouple of the same type. The absolute thermoelectric power of the samples was obtained after correction for the absolute thermopower of the Au leads, by using the data of Huebener.³⁶ In a second step, two additional contacts were placed to achieve a four-in-line contact configuration to perform electrical resistivity measurements. In the case of more conducting samples, a low-frequency AC method (77 Hz) was used, with a SRS model SR83 lock-in amplifier and applying a 1–5 μA current; for more resistive samples, a DC method was employed instead, using a Keithley 224 current source to apply through the sample both direct and reverse DC currents, well below 0.1 μA , and Keithley 619 electrometer to measure the corresponding voltage drop. Resistivity measurements under high hydrostatic pressure single crystals of **3** (phase 1) were performed in a NiCrAl clamped cell up to 2.7 GPa with silicone oil as the pressure transmitting medium. The pressure at room temperature was monitored with the resistance of a Manganin gauge located in the pressure cell. The pressure cell was then cooled down in a helium cryostat down to 4 K. The loss of pressure during cooling has been neglected as the applied pressures 2 and 2.7 GPa are close to the freezing pressure of the pressure medium at room temperature. The sample resistance was measured in 4 points with the low-frequency AC method applying a 10 μA current and using a lock-in amplifier EGG 5210 for detection.

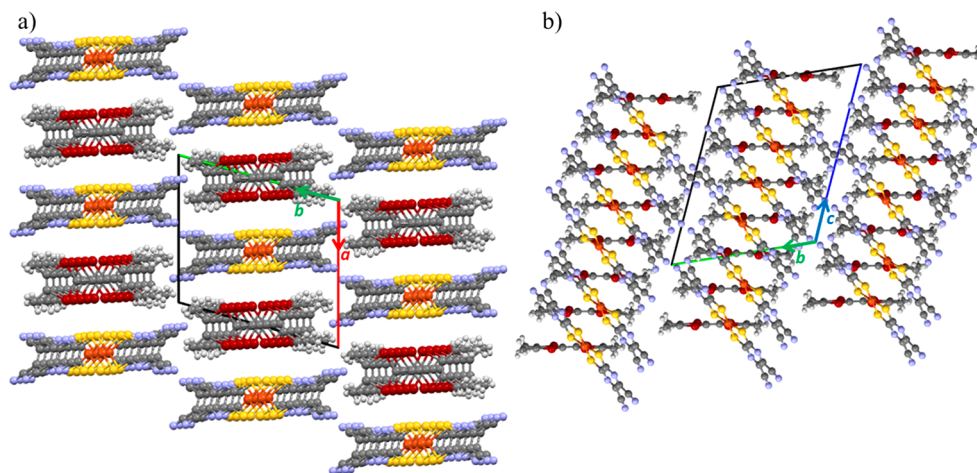


Figure 2. Crystal structure of $(\text{TMTSF})_5[\text{Cu}(\text{dcdmp})_2]_4$ (1): (a) view along c and (b) partial view of the stacks along the a axis.

RESULTS AND DISCUSSION

Electrocrystallization combining the electron donor molecules TMTSF and TTF with tetrabutylammonium salts of the electron acceptor molecules $[\text{M}(\text{dcdmp})_2]^{n-}$ ($n = 1$ for $\text{M} = \text{Au}$ and Cu ; $n = 2$ for $\text{M} = \text{Ni}$) resulted in four new charge transfer salts: $\text{TMTSF}_5[\text{Cu}(\text{dcdmp})_2]_4$ (1), $\text{TMTSF}_2[\text{Ni}(\text{dcdmp})_2]_2$ (2), $\text{TTF}_7[\text{Au}(\text{dcdmp})_2]_6$ (3), and $\text{TTF}_7[\text{Cu}(\text{dcdmp})_2]_6$ (4). Quality single crystals, suitable for single crystal X-ray diffraction studies and electrical transport properties measurements, were obtained. Table 1 summarizes the crystal and structural refinement data for compounds 1–4.

$(\text{TMTSF})_5[\text{Cu}(\text{dcdmp})_2]_4$ (1) crystallizes in the triclinic system, space group $P\bar{1}$ (Table 1). The asymmetric unit is composed of three independent TMTSF molecules, two (A and B) at general positions and one (C) at an inversion center, and two $[\text{Cu}(\text{dcdmp})_2]^-$ units both at general positions (D and E) (Tables S1 and S2). The donor molecules A and B present a small boat type distortion, while molecule C is within experimental error planar (Figure 1). The two acceptor molecules D and E show a small chair-type distortion with molecule D displaying a very small tetrahedral distortion of the central coordination sulfur atoms (Figure 1). Each donor molecule (A, B, and C) presents slightly different bond lengths. A bond length analysis using a comparison with well-known TMTSF salts^{37–39} as shown in Tables S3 and S4 suggests that, whereas molecule A is partially oxidized with a +0.5 charge, molecules B and C are fully oxidized (Table S3). As for the acceptor molecules D and E, although crystallographically distinct, the bond length analysis is consistent in both cases with the same monoanionic state, $[\text{Cu}(\text{dcdmp})_2]^-$ (Table S4).

The crystal structure of $(\text{TMTSF})_5[\text{Cu}(\text{dcdmp})_2]_4$ (1), as shown in Figure 2, is composed of an herringbone arrangement of segregated stacks of donors and acceptors molecules along c . The angle of the molecular average planes between donor and acceptor stacks is $\sim 56.1(1)^\circ$. The stacks are however far from being regular. The donors are arranged with the repeat unit $\dots \text{A}^{0.5+}\text{B}^+\text{C}^+\text{B}^+\text{A}^{0.5+}\dots$, and the molecules are slipped along their major axis by about 1.5 Å with overlap modes depicted in (Figure 3). The average mean interplanar distances are 3.543(5) Å, 3.742(5) Å, and 3.710(5) Å between molecules A–A, A–B, and B–C, respectively. The good overlap of the donors within the stacks and the short interplanar distances indicate the existence of strong donor–donor intrastack π – π interactions. Several short intrastack $\text{Se}\cdots\text{Se}$ (3.85–3.88 Å)

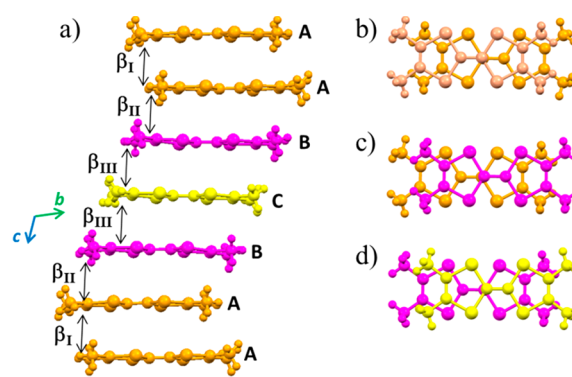


Figure 3. Partial view of the donors in the crystal structure of $(\text{TMTSF})_5[\text{Cu}(\text{dcdmp})_2]_4$ (1): (a) side view of a donor stack, (b–d) overlap modes of molecules A–A (b), A–B (c), and B–C (d).

contacts can be observed between molecules A–A and B–C, comparable to those observed in molecular conductors TMTSF-TCNQ (3.88 Å) and TMTSF-DMTCNQ (3.94 Å) (Table S5).³⁷ Between molecules A and B, the short contacts are through a $\text{C}-\text{H}\cdots\text{Se}$ hydrogen bond (Table S5). In the acceptor stacks, the anions are arranged with the repeat unit $\dots \text{D}^-\text{E}^-\text{D}^-\dots$, and the molecules are slipped both along their major and minor axis with overlap modes depicted in Figure 4. The average mean interplanar distances between molecules D–D, E–E, and D–E are 3.492(5) Å, 3.345(5) Å, and 3.222(5) Å, respectively, indicating the existence of strong π – π interactions within the acceptor stacks. Donor and acceptor molecules in neighboring stacks, along the a axis, are

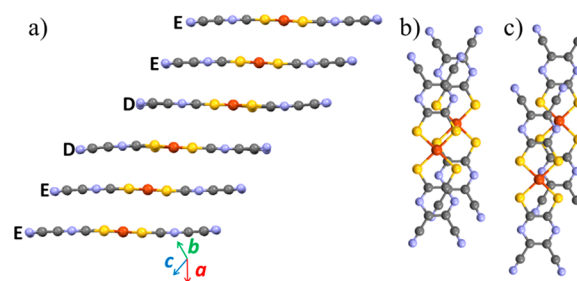


Figure 4. Partial view of the anions in the crystal structure of $(\text{TMTSF})_5[\text{Cu}(\text{dcdmp})_2]_4$ (1): (a) side view of an acceptor stack, (b–c) overlap modes of units D–E and E–E (b) and D–D (c).

connected by short Se...S and Se...N contacts, while along the *b* axis the molecules are connected by C–H...N hydrogen bonds (Table S5).

The [Cu(dcdmp)₂] units are in a monoanionic state, and therefore their stacks lead to filled bands with no contribution to the electrical conductivity, which should occur via the stacks of the partially oxidized donors. The electronic band structure associated with the donor stacks was analyzed under the extended Hückel approximation considering the HOMO–HOMO intermolecular interactions between TMTSF molecules in the stacks. There are three types of intermolecular TMTSF donor–donor interactions along the stacking axis: β_I between molecules A–A, β_{II} between molecules A–B and β_{III} between molecules B–C (Figure 3a). These interactions were estimated as 611, 568, and 590 meV respectively for β_I , β_{II} , and β_{III} . These are relatively large energy interactions of the same magnitude, which in the face of negligible interstack interactions predicts a relatively large wide band with strong one-dimensional (1D) character as depicted in Figure 5. The

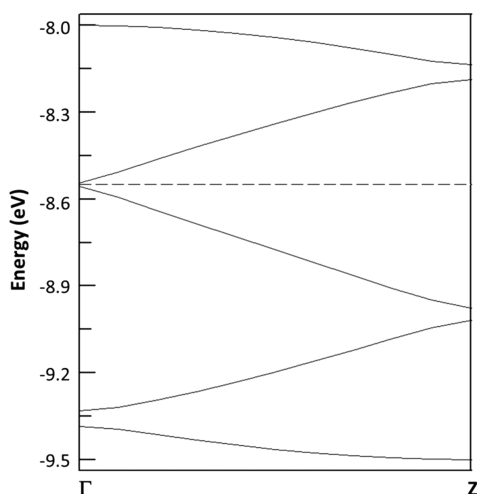


Figure 5. Calculated electronic band structure of **1** ($\Gamma = 0, 0, 0; Z = 0, 0, 1/2^*$). The Fermi level, E_F , is depicted as a dashed line.

HOMO of the five molecules in the unit cell leads to five bands separated by relatively small gaps as expected from identical values of β_{I-III} . Considering the average donor oxidation state (TMTSF)^{4/5+}, the Fermi level in the donor bands (dashed line in Figure 5) lies at a very small gap, and therefore quasi-metallic 1D properties are expected.

The small dimensions of TMTSF₂[Ni(dcdmp)₂] (**2**) crystals (0.08 × 0.03 × 0.01 mm³) precluded single crystal X-ray diffraction using diffractometers with conventional source (fine-focus sealed tube), and its crystal structure could only be obtained by using synchrotron radiation at ID11 at ESRF (2001). Compound **2** crystallizes in the monoclinic system, space group *P2₁/c* (Table 1). The unit cell contains one independent [Ni(dcdmp)₂]²⁻ complex and two independent TMTSF molecules (Table S6). While the Ni complex presents a slight chair type distortion, the TMTSF molecules present a slight boat type distortion due to a small deviation from the molecular plane of the terminal methyl groups (Figure 6). The average Ni–S bond length found in the acceptor (2.18(1) Å) clearly indicates that the complex is in a dianionic state (Table S7). The two crystallographic distinct donor molecules (A and B) present slightly different bond lengths, which are however within experimental uncertainty identical, and a clear

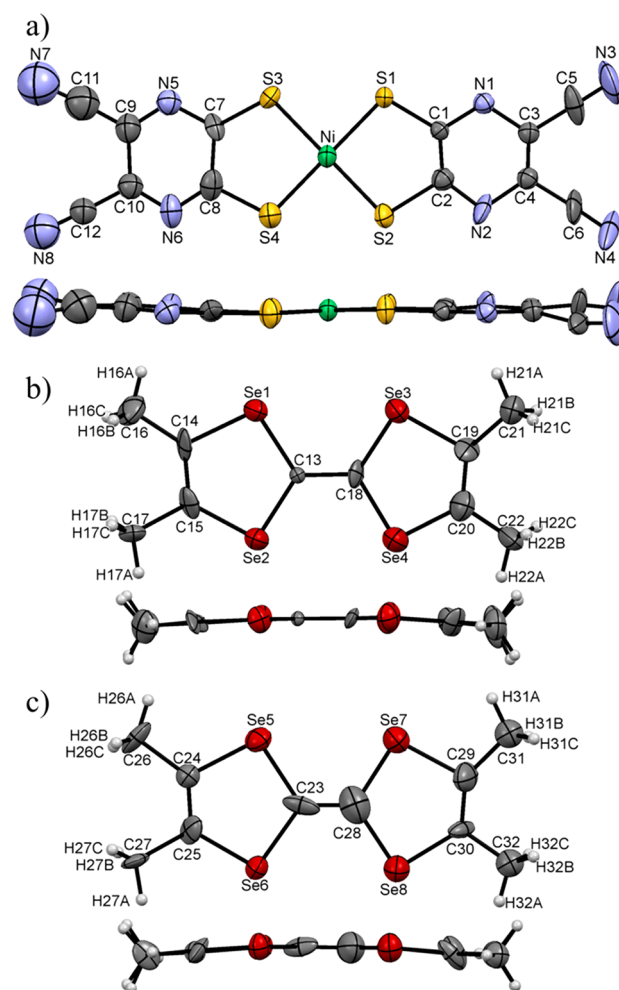


Figure 6. ORTEP and atomic numbering schemes (top and side views) of (a) [Ni(dcdmp)₂]²⁻, (b) TMTSF molecule A, and (c) TMTSF molecule B in compound **2**, with thermal ellipsoids at the 50% probability level.

attribution of the charge to each molecule could not be precise; nevertheless, this compound can be formulated as TMTSF₂⁺[Ni(dcdmp)₂]²⁻ (Table S8).

The crystal structure of TMTSF₂[Ni(dcdmp)₂] (**2**) is composed of mixed columns of face to face donor dimers and acceptors, ...((DD)²⁺A²⁻(DD)²⁺A²⁻)..., along the *c* axis (Figure 7) in a pattern similar that of related BET-TTF₂[Cu(dcdmp)₂].¹⁷ The donor dimers and the acceptor anionic molecules are positioned with an angle between average planes of 70.8(2)°. The molecules in the dimer present quite short Se...Se contacts (3.52–3.66 Å) (Table S9). Along the column the acceptor is connected to both TMTSF molecules in the dimers by short S...Se contacts. Along *b*, these columns are arranged out-of-registry and present S...Se short contacts, between donor and acceptor molecules, in a bi-dimensional network along the *b,c* plane. Along *a* axis, the only existent intermolecular contacts are C–H...N hydrogen bonds, involving a nitrogen atom of the acceptors cyanonitrile group and a hydrogen atom of the donors terminal methyl group (Table S9). Apart from the strong dimer interactions, all other interactions are among different species. This structure can also be described as being composed of TMTSF dimers surrounded by acceptors molecules.

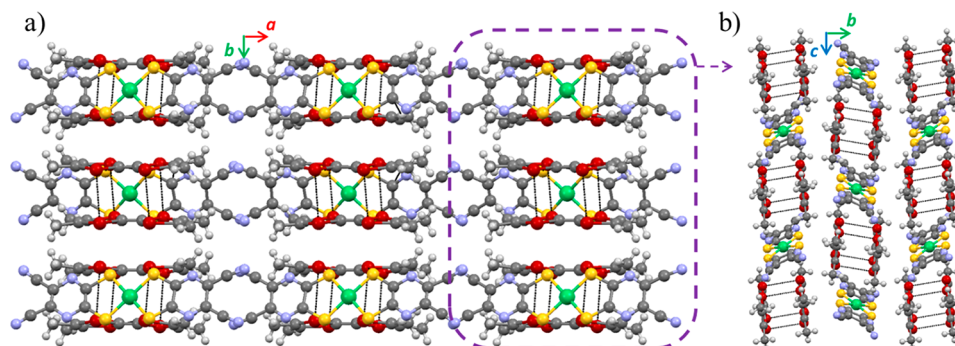


Figure 7. Crystal structure of (a) $(\text{TMTSF})_2[\text{Ni}(\text{dcdmp})_2]$ (2) along the c axis. (b) Partial view of the packing in the b,c plane with the alternating anions and TMTSF dimers.

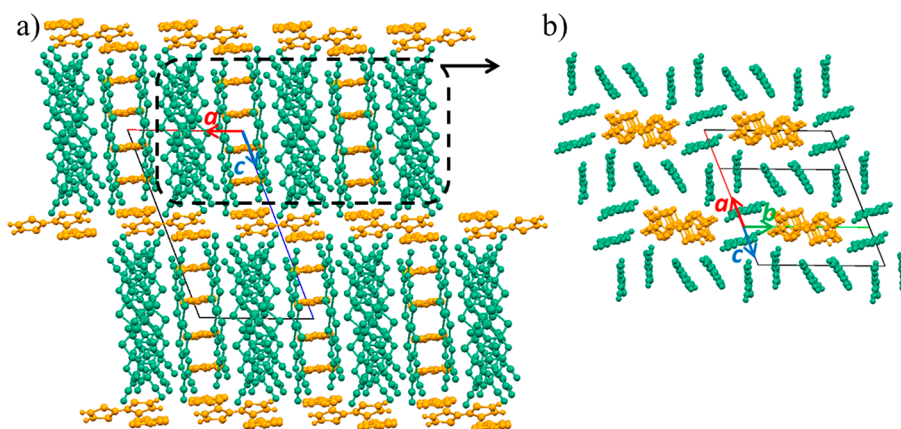


Figure 8. Crystal structure of $(\text{TTF})_7[\text{M}(\text{dcdmp})_2]_6$ ($\text{M} = \text{Au}$ (3) and Cu (4)): (a) view along b and (b) partial view of a layer with isolated piles of TTF donor surrounded by $[\text{M}(\text{dcdmp})_2]^-$ pairs.

$(\text{TTF})_7[\text{Au}(\text{dcdmp})_2]_6$ (3) and $(\text{TTF})_7[\text{Cu}(\text{dcdmp})_2]_6$ (4) were found to be isostructural, in spite of lower diffracting quality of the Cu salt, crystallizing in the triclinic system, space group $P\bar{1}$ (Table 1). The asymmetric unit is composed of four TTF donor molecules, molecules A, B, and C at general positions and molecule D at an inversion center, and three $[\text{M}(\text{dcdmp})_2]$ units (molecules E, F, and G) at general positions (Tables S10 and S11). TTF molecules A and B of compound 3 present a slight torsion angle on the central $\text{C}=\text{C}$ bond, while C has a small type boat distortion and D is planar within experimental error (Figure S1). The $[\text{Au}(\text{dcdmp})_2]$ molecules F and G have a small chair-type distortion, whereas E appears to be essentially planar, within experimental error. In compound 4 with lower quality structural refinement, the molecular distortions are identical (Figure S2). The ionic charge of these molecules could be estimated through a bond length analysis, which in these cases confirmed the monoanionic state of $[\text{Cu}(\text{dcdmp})_2]$ and $[\text{Au}(\text{dcdmp})_2]$, implying a total charge of +6 for the seven TTF molecules in the unit cell. Although the donor bond lengths clearly denote different degrees of oxidation, due to the lack of higher resolution, especially for the Cu complex, a clear attribution of a charge to each TTF molecule could not be unequivocally attributed (Tables S12 and S13).

The crystal structure of 3 and 4 is represented in Figure 8. These structures are composed of blocks of piled up TTF hexamers, ABCBA which, in the a,c plane, are surrounded by six pairs of parallel $[\text{M}(\text{dcdmp})_2]^-$ anions. Along c the blocks are interconnected by TTF molecule D. Within the TTF hexamers, the molecules are essentially parallel with overlap

modes shown in Figure 9, where relative to the A–B units, molecule C is shifted along their long molecular axis. The

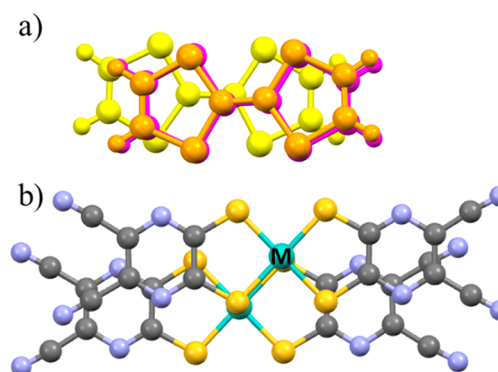


Figure 9. $(\text{TTF})_7[\text{M}(\text{dcdmp})_2]_6$ ($\text{M} = \text{Au}$ (3) and Cu (4)) overlap modes of (a) TTF units A (orange), B (pink), and C (yellow) and $[\text{M}(\text{dcdmp})_2]$ units (b).

mean intra-hexamer interplanar distances are between 3.37(2) and 3.65(2) Å, which are in the range of relatively short π – π interaction (3.3–3.8 Å).⁴⁰ Also, within the TTF hexamer stacks, the molecules are connected to each other by short $\text{S}\cdots\text{S}$ contacts (between A–B, B–C, and C–C). A network of short $\text{S}\cdots\text{S}$ and $\text{S}\cdots\text{N}$ contacts and hydrogen bonds connects the acceptor molecules (E, F, and G) to the TTF hexamers (Tables S14 and S15). The pairs of anions are connected by short $\text{S}\cdots\text{S}$ contacts. This network of short contacts is more

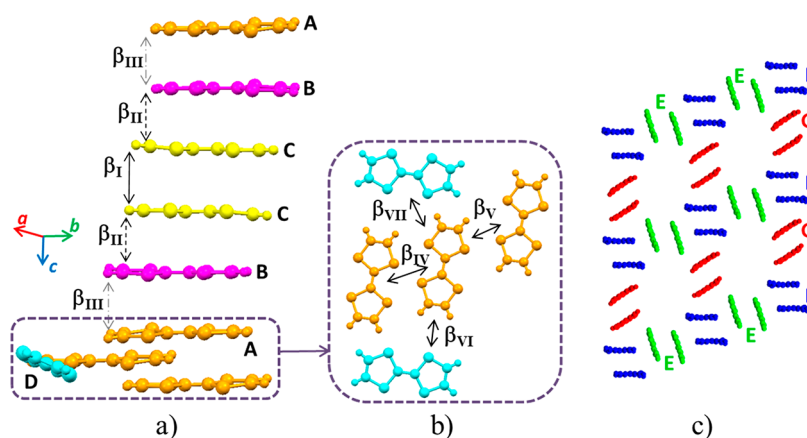


Figure 10. Crystal structure $(\text{TTF})_7[\text{M}(\text{dcdmp})_2]_6$ ($\text{M} = \text{Au}$ (3) and Cu (4)): (a, b) schematic representation of different TTF molecules and (c) $[\text{M}(\text{dcdmp})_2]$ units in the crystal packing.

Table 2. Intermolecular Energy Interactions β_I – β_{VII} (meV) between Donor Molecules Represented in Figure 10, in the Crystal Structure of $(\text{TTF})_7[\text{M}(\text{dcdmp})_2]_6$ ($\text{M} = \text{Au}$ (3) and Cu (4)), Estimated by the Extended Hückel Calculations Using a Double- ξ Approximation

CT salts	β (meV)						
	β_I	β_{II}	β_{III}	β_{IV}	β_V	β_{VI}	β_{VII}
$\text{TTF}_7[\text{Au}(\text{dcdmp})_2]_6$ (3)	−905	−477.8	−1223	185	−4.2	23.8	−9.6
$\text{TTF}_7[\text{Cu}(\text{dcdmp})_2]_6$ (4)	−918.8	−541.6	−1124.3	−146.2	−40.3	−17.6	−13.7

significant in the case of 4, where $\text{Au}\cdots\text{S}$ interactions are also observed (Tables S14 and S15).

The magnitude of the intermolecular interactions between TTF donor units in 3 and 4 were estimated by calculations based on the extended Hückel approximation using a double- ξ basis. In these structures, there are seven types of intermolecular TTF donor–donor interactions, three along the TTF hexamer columns (β_I – β_{III}) and four between the TTF molecules A of different hexamer columns and also with molecule D (β_{IV} – β_{VII}) (Figure 10a–b). Table 2 shows that both gold and copper compounds present similar intermolecular interaction energies, except for β_V that becomes negligible in the gold compound. The highest intermolecular interaction is found between molecules A–B (β_{III}), followed by the interaction between molecules C–C (β_I), which is probably due to the larger interplanar distance. Despite the uncertainty on the absolute values obtained by the calculations under this approach, the results provide a fair indication of their relative magnitude. The interactions between different hexamers are quite small when compared to the ones in the hexamer.

Compound 2 presents a structure with isolated donor dimers and therefore it is expected to be an insulator. Indeed, the measurements in single crystals reveal an insulating behavior with values of $\sim 6 \times 10^{-4}$ S/cm. This situation contrasts clearly with the case of compound 1, where the extended network of partially oxidized donor molecules suggests a priori a good candidate to exhibit high electrical conductivity. In compounds 3 and 4, the case is quite diverse as the network of partially oxidized donors seems to be essentially confined to the hexamers of TTF donors, and the existence of extended interactions between the donors would have to involve one TTF donor that appears to be relatively isolated in the crystal structure, displaying only rather weak interactions to the other donors. Nevertheless, it appears worthwhile to investigate the electrical transport properties of

the compounds 3 and 4 (that are expected to be less conductive than 1, but possibly more conductive than 2). The results of the electrical resistivity, ρ , and thermoelectric power, S , measurements as a function of temperature in single crystals of compounds 1, 3, and 4 are shown in Figure 11 and Table 3. $(\text{TMTSF})_5[\text{Cu}(\text{dcdmp})_2]_4$ (1) presents a rather high electrical conductivity ~ 134 S/cm at room temperature, with a very small temperature dependence at high temperatures down to approximately 110 K, while thermopower is rather small ($S_{\text{RT}} = -17$ $\mu\text{V}/\text{K}$), suggesting an almost metallic (slightly activated) regime as predicted by the band structure calculations mentioned before. Below ~ 110 K, there is a change of regime toward a semiconducting behavior with larger activation energy as seen both in the electrical resistivity and thermopower. This change of regime becomes more evident in the plot of the logarithmic derivative $d(\ln \sigma) / d(1000/T)$ (Figure 12a) presenting a sharp maximum at 110 K indicative of a structural transition associated with the increasing of a gap at the Fermi level. In view of the strong 1D character, this gap increase is possibly induced by a Peierls instability. This behavior is comparable to that previously reported for the analogous Au compound $\text{TMTSF}_m[\text{Au}(\text{dcdmp})_2]_n$ ¹⁵ with a smaller electrical conductivity, and for which a crystal structure could not be solved. It is worth mentioning that compound 1 has a structure reminiscent to that of TTF-TCNQ, with segregated donor and acceptor stacks, however with nonuniform stacking of the molecules in 1 the conductivity only occurring through the donor stacks. There are however significant differences from TTF-TCNQ that should be taken into account. First, the charge transfer between donors and acceptor stacks is commensurate, 4/5 (four electrons for each five donors), as dictated by the stoichiometry, while in TTF-TCNQ it is ca. 0.59. As a consequence of the monoanionic state of the acceptors in 1, their stacks lead to a completely filled band therefore without any contribution to the electrical conductivity, at variance with TTF-TCNQ where both donor

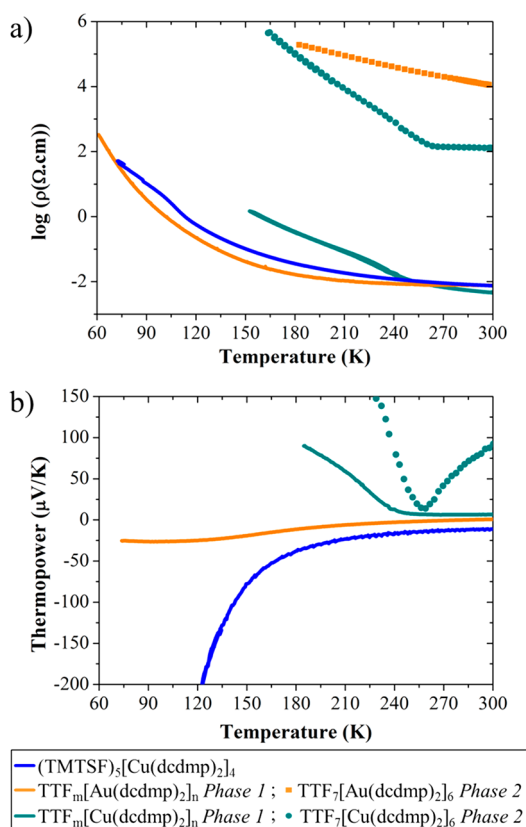


Figure 11. Temperature-dependent electrical resistivity (a) and thermoelectric power (b) of single crystals of (TMTSF)₅[Cu(dcdmp)₂]₄ (1) and (TTF)₇[M(dcdmp)₂]₆ (M = Au (3) and Cu (4)).

Table 3. Room-Temperature Electrical Conductivity (σ_{RT}) and Thermopower (S_{RT}) of Charge Transfer Salts 1–4 and Related Compounds in Single Crystals

CT salts	σ_{RT} (S/cm)	S_{RT} (μV/K)
(TMTSF) _m [Au(dcdmp) ₂] _n ¹⁵	13.4	−38
(TMTSF) ₅ [Cu(dcdmp) ₂] ₄ (1)	134	−17
(TMTSF) ₂ [Ni(dcdmp) ₂] (2)	6×10^{-4}	
(TTF) ₇ [Au(dcdmp) ₂] ₆ Phase 2 (3)	9×10^{-5}	
(TTF) _m [Au(dcdmp) ₂] _n Phase 1 (3) ¹⁵	100	0.6
(TTF) ₇ [Cu(dcdmp) ₂] ₆ Phase 2 (4)	7.7×10^{-3}	90
(TTF) _m [Cu(dcdmp) ₂] _n Phase 1 (4)	214	6

and acceptor bands have a contribution. Finally, in compound 1, the stacking of the molecules is not uniform, with the conducting donor stacks having a repeat of five molecules, therefore creating a small gap at the Fermi level.

In the electric transport properties of salts (TTF)₇[M(dcdmp)₂]₆ (M = Au (3) and Cu (4)), two different behaviors were observed, suggesting the existence of polymorphs or different stoichiometries (Figure 11). Evidence of different polymorphs was also observed in other previously reported salts with [M(dcdmp)₂] complexes (M = Au and Cu).^{17,41} We have defined the higher conducting behavior as phase 1 and the less conducting one as phase 2. It should be mentioned that the present data do not allow an unequivocal assignment of the stoichiometry to the different behaviors of the electrical transport properties. However, the observed structure for (TTF)₇[M(dcdmp)₂]₆ (3 and 4), with a quite irregular extension of electronic interactions, allowed us to assign it to

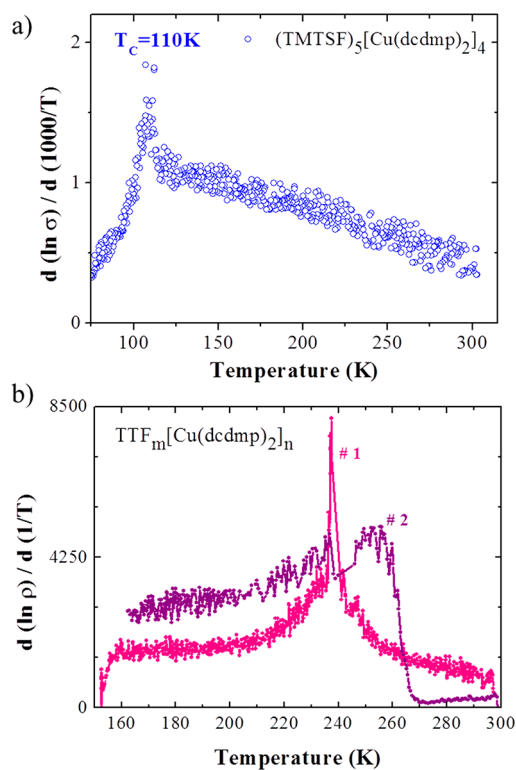


Figure 12. (a) Logarithmic derivative of electrical conductivity $d(\ln \sigma)/d(1000/T)$ versus temperature for (TMTSF)₅[Cu(dcdmp)₂]₄ (1) showing a maximum at 110 K. (b) Logarithmic derivative of electrical resistivity $d(\ln \rho)/d(1/T)$ versus temperature for phase 1 and 2 of (TTF)_m[Cu(dcdmp)₂]_n (4).

the less conducting phase (phase 2). In copper composition 4, we observed the less conducting phase 2 ($\sigma_{\text{RT}} = 7.7 \times 10^{-3}$ S/cm) following a semiconducting behavior, and a higher conducting phase 1 ($\sigma_{\text{RT}} = 214$ S/cm) with a transition around 240 K (Figure 11a), as denoted by the sharp maximum in the logarithmic derivative $d(\ln \rho)/d(1/T)$ (Figure 12b). This change of regime is also observed in the thermopower measurements, with small and almost temperature-independent values at higher temperatures until 240 K followed upon cooling by an increase of thermopower in a typical semiconducting behavior (Figure 11b). In the gold salt (3), a poor semiconducting behavior with a room temperature conductivity of 9×10^{-5} S/cm was observed in the so-called phase 2. This is at variance with that previously reported for (TTF)_m[Au(dcdmp)₂]_n, which presented a different unit cell of an unsolved structure and a more conducting behavior ($\sigma_{\text{RT}} = 100$ S/cm) (phase 1), therefore attributed to phase 1.¹⁵

The high electrical conductivity observed in phase 1 of (TTF)_m[Au(dcdmp)₂]_n motivated us to perform resistivity measurements under pressure (Figure 13) aiming at stabilizing a metallic state. Despite a significant and linear increase of the electrical conductivity with pressure at room temperature (usually indicative of a conducting regime in molecular materials), the temperature dependences of the resistivity, under 2 and 2.7 GPa applied pressures, still show a progressive localization. The thermal activation energy which can be determined below 200 K decreases with pressure from around 880 K (76 meV) at ambient pressure down to 375 K (32 meV) under 2.7 GPa (Figure 13). The room temperature thermopower of (TTF)_m[Au(dcdmp)₂]_n (3 phase 1) is nearly zero. When cooling down, it slowly decreases to negative values

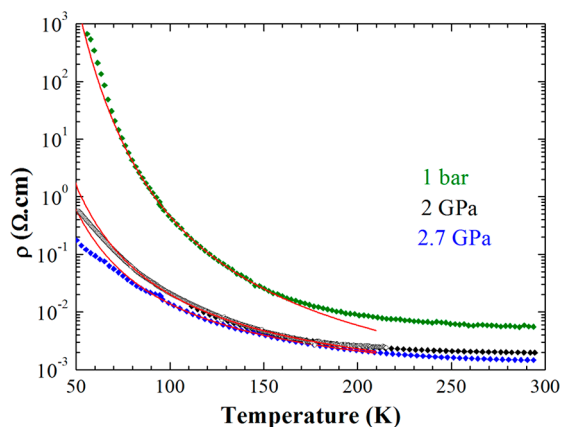


Figure 13. Electrical resistivity at different pressures of $(\text{TTF})_m[\text{Au}(\text{dcdmp})_2]_n$ (3 phase 1) single crystals as a function of temperature. The continuous red lines are the Arrhenius fit giving the activation energy at low temperature.

consistently with the progressive localization from a quasi-metallic regime at high temperature (Figure 11b).

CONCLUSION

The combination of the electron donors TMTSF or TTF with $[\text{M}(\text{dcdmp})_2]_n$ anions ($\text{M} = \text{Au}, \text{Cu}$ and Ni) led to new salts with interesting electric transport properties. The crystal structure analysis in compounds 1, 3, and 4 by single crystal X-ray diffraction revealed unusual stoichiometries. In the TTF-based compounds, electrical transport measurements in single crystals provide evidence of the existence of different phases, either polymorphism or different stoichiometries. In $\text{TMTSF}_5\text{-}[\text{Cu}(\text{dcdmp})_2]_4$ (1), the structure is composed of well segregated donor and acceptor stacks. The TMTSF stacks present large intermolecular interaction energies giving rise to high electrical conductivity at room temperature (134 S/cm) with quasi-metallic behavior and a transition to a semi-conducting state at 110 K. This compound can be compared to TTF-TCNQ considering that the contribution to the electrical conductivity comes only from the slightly modulated nonuniform donor stacks. Electrocrystallization experiments from TTF solutions in the presence of $[\text{M}(\text{dcdmp})_2]^-$ ($\text{M} = \text{Cu}$ and Au) anions provided crystals displaying two types of transport properties, phase 1 with a relatively high electrical conductivity and a phase 2 with semiconducting behavior. It was only possible to determine the crystal structure of the two isostructural compounds $(\text{TTF})_7[\text{M}(\text{dcdmp})_2]_6$ ($\text{M} = \text{Au}$ (3) and Cu (4)), and the crystal packing, although inconsistent with the behavior observed for phases 1, appears to be consistent with the semiconducting behavior of phase 2. Measurements with phase 1 $(\text{TTF})_m[\text{Cu}(\text{dcdmp})_2]_n$ crystals revealed a metal–insulator transition to occur at around 210 K. These results illustrate the rich variety of possible phases resulting from the combination of these anions with TTF type donors, with unusual structures and stoichiometries, associated with diverse electronic properties, including high electrical conductivity in spite of the structurally imposed modulation effects of the intermolecular electronic interactions.

ASSOCIATED CONTENT

Supporting Information

The Supporting Information is available free of charge on the ACS Publications website at DOI: 10.1021/acs.cgd.9b00958.

Tables of bond lengths and short contacts and figures of ORTEPs for compounds $\text{TMTSF}_5[\text{Cu}(\text{dcdmp})_2]_4$ (1), $\text{TMTSF}_2[\text{Ni}(\text{dcdmp})_2]_2$ (2), $\text{TTF}_7[\text{Au}(\text{dcdmp})_2]_6$ (3), and $\text{TTF}_7[\text{Cu}(\text{dcdmp})_2]_6$ (4) (PDF)

Accession Codes

CCDC 1940745–1940748 contain the supplementary crystallographic data for this paper. These data can be obtained free of charge via www.ccdc.cam.ac.uk/data_request/cif, or by emailing data_request@ccdc.cam.ac.uk, or by contacting The Cambridge Crystallographic Data Centre, 12 Union Road, Cambridge CB2 1EZ, UK; fax: +44 1223 336033.

AUTHOR INFORMATION

Corresponding Author

*E-mail: dbelo@ctn.tecnico.ulisboa.pt.

ORCID

Dulce Belo: 0000-0001-8480-963X

Notes

The authors declare no competing financial interest.

ACKNOWLEDGMENTS

This work was supported by FCT (Portugal) through Contracts UID/Multi/04349/2013, PTDC/QUI-QIN/29834/2017, and LISBOA-01-0145-FEDER-029666.

ABBREVIATIONS

dcdmp, 2,3-dicyano-5,6-dimercaptopyrazine; TCNQ, tetracyano-*p*-quinodimethane; TMTSF, tetramethyltetraselenafulvalene; TTF, tetrathiafulvalene

REFERENCES

- (1) Ferraris, J.; Cowan, D. O.; Walatka, V. V., Jr.; Perlstein, J. H. Electron Transfer in a New Highly Conducting Donor-Acceptor Complex. *J. Am. Chem. Soc.* **1973**, *95*, 948–949.
- (2) Bechgaard, K.; Cowan, D. O.; Bloch, A. N. Synthesis of the organic conductor tetramethyltetraselenofulvalenium 7,7,8,8-tetracyano-*p*-quinodimethanide (TMTSF-TCNQ)[4,4',5,5'-tetramethyl- Δ 2,2'-bis-1,3-diselenolium 3,6-bis-(dicyanomethylene)-cyclohexadienide]. *J. Chem. Soc., Chem. Commun.* **1974**, 937–938.
- (3) Williams, J. M.; Ferraro, J. R.; Thorn, R. J.; Carlson, K. D.; Geiser, U.; Wang, H. H.; Kini, A. M.; Whangbo, M.-H. *Organic Superconductors (Including Fullerenes): Synthesis, Structure, Properties, and Theory*; Prentice Hall, Englewood Cliffs, NJ, 1992.
- (4) Robertson, N.; Cronin, L. Metal bis-1,2-dithiolene complexes in conducting or magnetic crystalline assemblies. *Coord. Chem. Rev.* **2002**, *227*, 93–127.
- (5) Kagoshima, S.; Nagasawa, H. *One Dimensional Conductors*; Springer: Berlin, 2012; Vol. 72.
- (6) Valade, L.; Tanaka, H. Molecular Inorganic Conductors and Superconductors. In *Molecular Materials*; Bruce, D. W., O'Hare, D., Walton, R. I., Eds.; John Wiley & Sons Ltd: UK, 2010; pp 211–280.
- (7) Mori, T. *Electronic Properties of Organic Conductors*; Springer: Japan, 2013.
- (8) Brown, S. E. Organic superconductors: The Bechgaard salts and relatives. *Phys. C* **2015**, *514*, 279–289.
- (9) Mori, T. Organic Conductors with Unusual Band Fillings. *Chem. Rev.* **2004**, *104*, 4947–4969.
- (10) Oliveira, S.; Ministro, J.; Santos, I. C.; Belo, D.; Lopes, E.; Rabaça, S.; Canadell, E.; Almeida, M. Bilayer Molecular Metals Based on Dissymmetrical Electron Donors. *Inorg. Chem.* **2015**, *54*, 6677–6679.
- (11) Rabaça, S.; Almeida, M. Dithiolene complexes containing N coordinating groups and corresponding tetrathiafulvalene donors. *Coord. Chem. Rev.* **2010**, *254*, 1493–1508.

- (12) Simão, D.; Lopes, E. B.; Santos, I. C.; Gama, V.; Henriques, R. T.; Almeida, M. Charge Transfer Salts based on $\text{Cu}(\text{qdt})_2$, $\text{Ni}(\text{qdt})_2$ and $\text{Au}(\text{qdt})_2$ anions. *Synth. Met.* **1999**, *102*, 1613–1614.
- (13) Ribas, X.; Mas-Torrent, M.; Rovira, C.; Veciana, J.; Dias, J. C.; Alves, H.; Lopes, E. B.; Almeida, M.; Wurst, K. Molecular compounds based on DT-TTF and $\text{Au}(\text{cdc})_2$ complex. Structural, magnetic and electrical properties. *Polyhedron* **2003**, *22*, 2415–2422.
- (14) Neves, A. I. S.; Santos, I. C.; Belo, D.; Almeida, M. Cation and ligand roles in the coordination of Fe^{III} bisdithiolene complexes; the crystal structures of $(\text{BrBzPy})_2[\text{Fe}(\text{qdt})_2]_2$ and $[\text{Fe}(-\text{tpdt})_2]_2^{2-}$ salts. *CrystEngComm* **2009**, *11*, 1046–1053.
- (15) Belo, D.; Morgado, J.; Lopes, E. B.; Santos, I. C.; Rabaça, S.; Duarte, M. T.; Gama, V.; Henriques, R. T.; Almeida, M. Synthesis and Characterisation of Charge Transfer Salts Based on $\text{Au}(\text{dcdmp})_2$ and TTF Type Donors. *Synth. Met.* **1999**, *102*, 1751–1752.
- (16) Tomura, M.; Tanaka, S.; Yamashita, Y. Synthesis, structure and properties of the novel conducting dithiolato-metal complexes having dicyanopyrazine moieties. *Synth. Met.* **1994**, *64*, 197–202.
- (17) Silva, R. A. L.; Santos, I. C.; Rabaça, S.; Lopes, E. B.; Gama, V.; Almeida, M.; Belo, D. Synthesis and Characterization of Charge Transfer Salts Based on $[\text{M}(\text{dcdmp})_2]$ ($\text{M} = \text{Au}, \text{Cu}$ and Ni) with TTF Type Donors. *Crystals* **2018**, *8*, 141–157.
- (18) Belo, D.; Figueira, M. J.; Santos, I. C.; Gama, V.; Pereira, L. C.; Henriques, R. T.; Almeida, M. Synthesis and characterization of copper complexes with the 2,3-dicyano-5,6-dimercaptopyrazine ligand: Magnetic properties of a ferrocenium salt. *Polyhedron* **2005**, *24*, 2035–2042.
- (19) Belo, D.; Santos, I. C.; Almeida, M. 5,6-Dicyano-2,3-dithiopyrazine (dcdmp) chemistry: synthesis and crystal structure of $\text{Au}(\text{III})(\text{dcdmp})_2$ complexes and 2,3,7,8-tetracyano-1,4,6,9-tetraazothianthrene. *Polyhedron* **2004**, *23*, 1351–1359.
- (20) Perrin, D. D.; Armarego, W. L. F. *Purification of Laboratory Chemicals*; Pergamon Press: Exeter, 1988.
- (21) Sheldrick, G. M. SADABS; Bruker AXS Inc.: Madison, Wisconsin, USA, 2004.
- (22) SMART and SAINT; Bruker AXS Inc.: Madison, Wisconsin, USA, 2008.
- (23) Fair, C. K. *MoIEN. An Interactive Intelligent System for Crystal Structure Analysis*; Enraf-Nonius: Delft, Netherlands, 1990.
- (24) Altomare, A.; Burla, M. C.; Camalli, M.; Cascarano, G.; Giacovazzo, G.; Guagliardi, A.; Moliterni, A. G. G.; Polidori, G.; Spagna, R. SIR97: a new tool for crystal structure determination and refinement. *J. Appl. Crystallogr.* **1999**, *32*, 115–119.
- (25) Sheldrick, G. M. A short history of SHELX. *Acta Crystallogr., Sect. A: Found. Crystallogr.* **2008**, *A64*, 112–122.
- (26) Farrugia, L. J. WinGX and ORTEP for Windows: an update. *J. Appl. Crystallogr.* **2012**, *45*, 849–854.
- (27) Macrae, C. F.; Bruno, I. J.; Chisholm, J. A.; Edgington, P. R.; McCabe, P.; Pidcock, E.; Rodriguez-Monge, L.; Taylor, R.; van de Streek, J.; Wood, P. A. Mercury CSD 2.0-new features for the visualization and investigation of crystal structures. *J. Appl. Crystallogr.* **2008**, *41*, 466–470.
- (28) Ren, J.; Liang, W.; Whangbo, M.-H. *Crystal and Electronic Structure Analysis Using CAESAR*; PrimeColor Software: USA, 1998. <http://www.primec.com/index.htm>.
- (29) Hoffmann, R. An Extended Hückel Theory. I. Hydrocarbons. *J. Chem. Phys.* **1963**, *39*, 1397–1412.
- (30) Whangbo, M.-H.; Hoffmann, R. The band structure of the tetracyanoplatinate chain. *J. Am. Chem. Soc.* **1978**, *100*, 6093–6098.
- (31) Whangbo, M.-H.; Hoffmann, R.; Woodward, R. B. Conjugated One and Two Dimensional Polymers. *Proc. R. Soc. London, Ser. A* **1979**, *366*, 23–46.
- (32) Canadell, E.; Rachidi, I.E.-I.; Ravy, S.; Pouget, J. P.; Brossard, L.; Legros, J. P. On the band electronic structure of $\text{X}[\text{M}(\text{dmit})_2]_2$ ($\text{X} = \text{TTF}, (\text{CH}_3)_4\text{N}$; $\text{M} = \text{Ni}, \text{Pd}$) molecular conductors and superconductors. *J. Phys. (Paris)* **1989**, *50*, 2967–2981.
- (33) Chaikin, P. M.; Kwak, J. F. Apparatus for thermopower measurements on organic conductors. *Rev. Sci. Instrum.* **1975**, *46*, 218–220.
- (34) Almeida, M.; Alcácer, L.; Oostra, S. Anisotropy of thermopower in N-methyl-N-ethylmorpholinium bistetracyanoquinodimethane, $\text{MEM}(\text{TCNQ})_2$, in the region of the high-temperature phase transitions. *Phys. Rev. B: Condens. Matter Mater. Phys.* **1984**, *30*, 2839–2844.
- (35) Lopes, E. B. INETI-Sacavém, Internal Report, Portugal, 1991.
- (36) Huebener, R. P. Thermoelectric Power of Lattice Vacancies in Gold. *Phys. Rev.* **1964**, *135*, A1281–A1291.
- (37) Kistenmacher, T. J.; Emge, T. J.; Shu, P.; Cowan, D. O. 4,4',5,5'-Tetramethyl->2',2'-bis-1,3-diselenole, TMTSF. *Acta Crystallogr., Sect. B: Struct. Crystallogr. Cryst. Chem.* **1979**, *35*, 772–775.
- (38) Thorup, N.; Rindorf, G.; Soling, H.; Bechgaard, K. The Structure of $\text{Di}(2,3,6,7\text{-tetramethyl-1,4,5,8-tetraselenafulvalenium})\text{Hexafluorophosphate}^*$ ($\text{TMTSF})_2\text{PF}_6$, the First Superconducting Organic Solid. *Acta Crystallogr., Sect. B: Struct. Crystallogr. Cryst. Chem.* **1981**, *37*, 1236–1240.
- (39) Chang, H.-C.; Kitagawa, S.; Kondo, M.; Ishii, T. Structural, Spectroscopic and Magnetic Properties of Charge-Transfercomplex, $(\text{TMTSF})[\text{Cr}(\text{Cl}_4\text{SQ})_2(\text{Cl}_4\text{Cat})] \bullet 0.5\text{SCH}_2\text{Cl}_2$. *Mol. Cryst. Liq. Cryst. Sci. Technol., Sect. A* **1999**, *335*, 183–192.
- (40) Janiak, C. A critical account on π - π stacking in metal complexes with aromatic nitrogen-containing ligands. *J. Chem. Soc., Dalton Trans.* **2000**, 3885–3896.
- (41) Silva, R. A. L.; Santos, I. C.; Lopes, E. B.; Rabaça, S.; Gancedo, J. V.; Rovira, C.; Almeida, M.; Belo, D. DT-TTF Salts with $[\text{Cu}(\text{dcdmp})_2]^-$: The Richness of Different Stoichiometries. *Cryst. Growth Des.* **2016**, *16*, 3924–3931.